



Film Thickness Formula for Thermal EHL Line Contact Considering a New Reynolds–Carreau Equation

Eduardo de la Guerra Ochoa¹ · Javier Echávarri Otero¹ · Alejandro Sánchez López¹ · Enrique Chacón Tanarro¹ · Benito del Río López²

Received: 6 October 2017 / Accepted: 4 January 2018 / Published online: 18 January 2018
© Springer Science+Business Media, LLC, part of Springer Nature 2018

Abstract

This article presents thermal EHL calculations for line contacts using a new analytical form of the Reynolds equation for lubricants whose rheological behaviour follows a modified Carreau model proposed by Bair. The isothermal calculation process was presented in: de la Guerra (Tribol Int 82:133–141, 2015). A new parametric formula is hereby developed using the aforementioned Reynolds–Carreau equation and adding the thermal effects to the solving process. The accuracy of this formula is discussed by comparing the estimates with the experimental and numerical results available. This analytical formula provides a fast and easy calculation methodology with good accuracy within a reasonably wide range of operating conditions.

Keywords Reynolds–Carreau equation · Shear-thinning · Thermal effects · Film thickness

List of symbols

a	Hertzian contact half-width (m)	p_0	Maximum Hertz pressure (Pa)
c_1	Specific heat of the lubricant (J/kg K)	Q	Flow rate per unit length (m ² /s)
c_b	Specific heat of the bodies (J/kg K)	R	Reduced contact radius (m)
$d_{1,2}$	Thermally affected depth of the bodies (m)	\bar{R}	Anuradha and Kumar factor for shear-thinning under pure rolling conditions
E'	Young's reduced modulus (Pa)	\bar{S}	Anuradha and Kumar factor for shear-thinning under rolling and sliding conditions
G	Shear modulus (Pa)	T	Temperature of the lubricant (K)
\bar{G}	Dimensionless material parameter	T_0	Reference temperature of the lubricant (K)
h	Film thickness profile (m)	T_1	Temperature of the upper body (K)
h_N	Newtonian central film thickness (m)	T_2	Temperature of the lower body (K)
h_0	Central film thickness (m)	T_b	Lubricant bath temperature (K)
k_1	Thermal conductivity of the lubricant (W/m K)	u	Velocity of the lubricant (m/s)
k_b	Thermal conductivity of the bodies (W/m K)	\bar{U}	Dimensionless velocity parameter
L	Contact length in flow direction (m)	$u_{1,2}$	Velocity of the surfaces (m/s)
L_T	Thermal loading factor	u_m	Average velocity of the contacting surfaces (m/s)
n	Carreau exponent	Δu	Sliding velocity of the contacting surfaces (m/s)
p	Pressure (Pa)	W	Normal load per unit length (N/m)
p_m	Average Hertz pressure (Pa)	\bar{W}	Dimensionless load parameter
		x	Coordinate in flow direction (m)
		z	Coordinate across the film thickness (m)
		α	Viscosity–pressure coefficient (Pa ⁻¹)
		β	Viscosity–temperature coefficient (K ⁻¹)
		$\dot{\gamma}$	Shear rate (s ⁻¹)
		ε	Thermal expansion coefficient (K ⁻¹)

✉ Eduardo de la Guerra Ochoa
e.delaguerra@upm.es

¹ Grupo de Investigación en Ingeniería de Máquinas, Universidad Politécnica de Madrid, José Gutiérrez Abascal 2, 28006 Madrid, Spain

² Física Aplicada e Ingeniería de los Materiales, Universidad Politécnica de Madrid, José Gutiérrez Abascal 2, 28006 Madrid, Spain

η	Viscosity (Pa s)
κ	Shear-thinning parameter
μ	Low-shear viscosity (Pa s)
μ_0	Low-shear viscosity at ambient pressure and reference temperature (Pa s)
ρ_l	Density of the lubricant (kg/m ³)
ρ_b	Density of the bodies (kg/m ³)
Σ	$\Delta u/u_m$, slide-to-roll ratio
τ	Shear stress (Pa)
τ_m	Mid-plane shear stress (Pa)
φ_{NN}	Shear-thinning factor under pure rolling conditions
φ_{SRR}	Shear-thinning factor under rolling and sliding conditions
φ_T	Thermal film thickness factor

$$\eta = \mu \left(1 + \left(\frac{\tau}{G} \right)^2 \right)^{\frac{(1-(1/n))}{2}} \tag{2}$$

where low-shear viscosity is assumed to vary exponentially with pressure and temperature [6], according to Eq. (3)

$$\mu = \mu_0 e^{(\alpha p - \beta(T - T_0))} \tag{3}$$

The Carreau equation incorporates the variation in the viscosity–temperature and the viscosity–pressure coefficients under shear-thinning conditions.

De la Guerra et al. [7] presented a new analytical form (4) of the one-dimensional Reynolds equation for lubricants whose rheological behaviour fits the modified Carreau model proposed by Bair

$$Q = u_1 h - \frac{G^{(n-1)/n} n \left(G^2 + \left(\tau_m - \frac{\partial p}{\partial x} \frac{h}{2} \right)^2 \right)^{\frac{1+n}{2n}} h}{(1+n)\mu \frac{\partial p}{\partial x}} + \frac{nG^2 \left(\tau_m + \frac{\partial p}{\partial x} \frac{h}{2} \right)}{(1+n)\mu \left(\frac{\partial p}{\partial x} \right)^2} \text{hypergeom} \left(\left[\frac{1}{2}, -\frac{1+n}{2n} \right], \left[\frac{3}{2} \right], -\frac{\left(\tau_m + \frac{\partial p}{\partial x} \frac{h}{2} \right)^2}{G^2} \right) - \frac{nG^2 \left(\tau_m - \frac{\partial p}{\partial x} \frac{h}{2} \right)}{(1+n)\mu \left(\frac{\partial p}{\partial x} \right)^2} \text{hypergeom} \left(\left[\frac{1}{2}, -\frac{1+n}{2n} \right], \left[\frac{3}{2} \right], -\frac{\left(\tau_m - \frac{\partial p}{\partial x} \frac{h}{2} \right)^2}{G^2} \right) \tag{4}$$

1 Introduction

Generalised Reynolds equations are largely used to determine elastohydrodynamic film thickness for shear-thinning lubricants [1, 2]. Very often, the rheological behaviour of the lubricants is properly described by the Carreau model [3], which is formulated in Eq. (1)

$$\eta = \mu \left(1 + \left(\frac{\mu \dot{\gamma}}{G} \right)^2 \right)^{\frac{(n-1)}{2}} \tag{1}$$

When dealing with generalised Reynolds equations for non-Newtonian fluids, a modified version is frequently used, with τ being the independent variable. Bair [4, 5] proposed Eq. (2), valid for $0.2 < n < 1$, which is therefore applicable to most non-Newtonian fluids that follow the Carreau model

where *hypergeom* denotes the Gauss hypergeometric function. Equation (4) is a function of τ_m (the value of the shear stress at the lubricant mid-plane), which is calculated with Eq. (5)

$$\frac{(u_2 - u_1)\mu \frac{\partial p}{\partial x} (1+n)}{G^{1-(1/n)n}} = \left(G^2 + \tau_m^2 + \tau_m h \frac{\partial p}{\partial x} + \frac{1}{4} \left(h \frac{\partial p}{\partial x} \right)^2 \right)^{\frac{1+n}{2n}} - \left(G^2 + \tau_m^2 - \tau_m h \frac{\partial p}{\partial x} + \frac{1}{4} \left(h \frac{\partial p}{\partial x} \right)^2 \right)^{\frac{1+n}{2n}} \tag{5}$$

Other forms of Reynolds–Carreau equations have also been developed for line contacts [6, 8]. The formulation proposed by Bair [8] is based on numerical adjustment of the equations for flow-rate and mid-plane shear stress through simulations under different operating conditions. Unlike the approximate expression attained in that way, the new Reynolds–Carreau equation [7] was obtained in a general manner

by adding the shear-thinning influence to a procedure similar to that used for deducing the classic Reynolds equation.

All these approaches greatly simplify the solving process. The use of Grubin-style calculations [9] has shown to provide quick and reasonably accurate results of the shear-thinned central film thickness under isothermal conditions [8, 10]. In contrast, the use of full EHL solving methods involves a very high computational cost.

On the other hand, bearing in mind a practical use of the film thickness results, several formulae have been deduced from a regression using data from full EHL calculations. By the way of example, Anuradha and Kumar developed accurate expressions for the central film thickness [2, 10] shown in Eqs. (6–9), which are used as reference values in the present article

$$\frac{h_0}{R} = 1.904093 \bar{U}^{-0.696} \bar{G}^{-0.562} \bar{W}^{-0.144} \bar{RS} \tag{6}$$

where

$$\bar{U} = \frac{\mu_0 u_m}{E'R}; \quad \bar{G} = \alpha E'; \quad \bar{W} = \frac{W}{E'R} \tag{7}$$

$$\bar{R} = \left(1 + 0.122459 \frac{\bar{U}^{-0.453} \bar{W}^{-0.27}}{\bar{G}^{-0.22} (G/E')^{1.288}} \right)^{-1.2(1-n)^{1.44}} \tag{8}$$

$$\bar{S} = \left(1 + 1.08 \frac{\Sigma^{2.22} \bar{U}^{-0.047} \bar{W}^{-0.03}}{\bar{G}^{-0.176} (G/E')^{0.11}} \right)^{-1.3(1-n)^{1.6}} \tag{9}$$

Another remarkable approach based on numerical EHL calculations and the ensuing regression analysis is the shear-thinning parameter κ proposed by Bair [6] and shown in Eq. (10), which divides the Newtonian central film thickness to obtain the corresponding value under shear-thinning conditions

$$\kappa = \left[1 + 0.79 \left((1 + \Sigma) \frac{u_m \mu_0}{h_N G} \right)^{\frac{1}{1+0.2\Sigma}} \right]^{3.6(1-n)^{1.7}} \tag{10}$$

In addition, the heat generated in the contact can cause a local rise in the lubricant temperature, especially for high slide-to-roll ratios (SRRs), leading to a reduction in film thickness. Based on Cheng, Gupta and other authors, Hamrock proposed a correction factor (11) that can be applied to the isothermal film thickness to take into account the thermal effects [11, 12]

$$\varphi_T = \frac{1 - 13.2(p_0/E')L_T^{0.42}}{1 + 0.213 \left[1 + 2.23 \left(\frac{\Delta u}{u_m} \right)^{0.83} \right] L_T^{0.64}}; \quad \text{where} \quad L_T = \frac{\beta \mu_0 u_m^2}{k_1} \tag{11}$$

More recently, Anuradha and Kumar [13] analysed several cases and reported a significant influence not only of shear-thinning but also of thermal effects on film thickness.

Besides the existing predictions for thermal film thickness based on simple formulae, the thermal influence is frequently considered by means of the energy equation [14], solved together with generalised Reynolds equations. This involves an additional increase in the computational cost. The general expression for the energy equation in line contact is as follows [14]

$$\frac{\partial}{\partial x} \left(k_1 \frac{\partial T}{\partial x} \right) + \frac{\partial}{\partial z} \left(k_1 \frac{\partial T}{\partial z} \right) + \varepsilon Tu \frac{\partial p}{\partial x} + \eta \left(\frac{\partial u}{\partial z} \right)^2 = \rho_1 c_1 u \frac{\partial T}{\partial x} \tag{12}$$

The thermal balance for each contacting body i ($i = 1, 2$) is given by Eq. (13),

$$\frac{\partial^2 T_{1,2}}{\partial x^2} + \frac{\partial^2 T_{1,2}}{\partial z^2} = \frac{\rho_b c_b}{k_b} u_{1,2} \frac{\partial T_{1,2}}{\partial x} \tag{13}$$

The following assumptions are frequently made:

- Couette flow, with a negligible Poiseuille component [6].
- All heat generated by fluid shear (none by compression) [15].
- Absence of heat conduction in the x -direction within the lubricant film and the contacting bodies [16, 17].
- Thermal properties of the lubricant and contacting bodies constant with temperature [18].

Thus, Eqs. (12) and (13) are simplified as follows

$$k_1 \frac{\partial^2 T}{\partial z^2} + \eta \left(\frac{\partial u}{\partial z} \right)^2 = \rho_1 c_1 u \frac{\partial T}{\partial x} \tag{14}$$

$$\frac{\partial^2 T_{1,2}}{\partial z^2} = \frac{\rho_b c_b}{k_b} u_{1,2} \frac{\partial T_{1,2}}{\partial x} \tag{15}$$

In this article, central film thickness and temperature distribution are calculated by adding thermal considerations to the Reynolds–Carreau equations proposed in references [8, 10] for line contacts.

It is generally accepted that the central film thickness is essentially determined by the fluid dynamics of the inlet zone, irrespective of the lubricant behaviour within the Hertz region [6, 14]. This characteristic greatly simplifies the solving process when compared with full thermal EHL simulations thanks to the Grubin inlet zone approximation for solving the Reynolds–Carreau equation, subsequently only requiring the need to solve the energy equation in the inlet zone.

Taking into account the results obtained, the new approach allows for a new formula to be developed to predict film thickness considering both shear-thinning and thermal effects. The new equation attempts to provide fast and reliable film thickness results by means of easy-to-use factors.

2 Calculating Film Thickness and Temperature Distribution

Reference [10] discloses the calculation of the isothermal film thickness, i.e. the equations involved, their discretization and the solving method. Hereby we aim to use an analogous process for calculating thermal film thickness. Consequently, a similar grid is selected in the flow direction x , from $x = -6a$ to the inlet $x = 0$. Each x -coordinate in the grid includes thirteen nodes in the z -direction: nine within the lubricant, two more in the fluid–solid interfaces and one additional node inside each contacting body at a depth equal to the thermally affected distance. Figure 1 shows the non-uniform grid selected for the lubricant.

The thermally affected distance represents the depth to which there is a thermal gradient in each body [19]. These depths can be calculated with Eq. (16)

$$d_{1,2} = \sqrt{\frac{k_b}{\rho_b c_b} \frac{dx}{u_{1,2}}} \tag{16}$$

Regarding the boundary conditions, the temperatures of the lubricant and the bodies are considered equal to the bath temperature T_b sufficiently far upstream (at a distance $6a$ to the inlet) and also for the bodies at depths equal to the thermally affected distances (d_1, d_2). Thus, the boundary conditions can be written as follows [20]

$$\begin{aligned} T(x = -6a, z) &= T_1(x = -6a, z) = T_2(x = -6a, z) = T_b, \quad \forall z \\ T_1(x, z = h/2 + d_1) &= T_b, \quad \forall x \\ T_2(x, z = -h/2 - d_2) &= T_b, \quad \forall x \end{aligned} \tag{17}$$

Continuity of heat flux and temperature is imposed across the two lubricant–solid interfaces. When the heat flow has

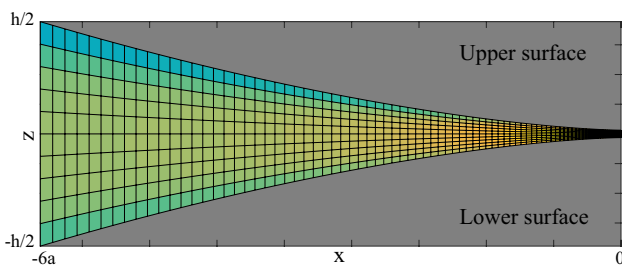


Fig. 1 Distribution of the nodes in the non-uniform grid

reached the bodies in contact, it is diffused to the inside of the bodies

$$\begin{aligned} k_1 \left(\frac{\partial T(x, z)}{\partial z} \right)_{z=h/2} &= k_b \frac{T_1(x, z = h/2) - T_b}{d_1}, \quad \forall x \\ k_1 \left(\frac{\partial T(x, z)}{\partial z} \right)_{z=-h/2} &= k_b \frac{T_2(x, z = -h/2) - T_b}{d_2}, \quad \forall x \end{aligned} \tag{18}$$

where

$$\begin{aligned} T_1(x, z = h/2) &= T(x, z = h/2), \quad \forall x \\ T_2(x, z = -h/2) &= T(x, z = -h/2), \quad \forall x \end{aligned} \tag{19}$$

Temperature gradients inside the bodies are not analysed in detail, as they are not relevant for the film thickness determination. However, the calculation process ensures that the energy equations are satisfied.

In addition to the equations exposed in Ref. [10], the discretization of the energy Eqs. (12, 13), together with their boundary conditions, is performed in line with Ref. [20].

Later on, we can solve the system of equations following the flow chart depicted in Fig. 2, attaining the temperature field and the thermal film thickness h_0 .

In the first step, the temperature is set equal to that of the lubricant bath, i.e. the temperature at a distance L sufficiently remote from the inlet: $L = 6a$. Applying the calculation method disclosed in Ref. [10], a velocity field and a film thickness are attained for the isothermal case, which

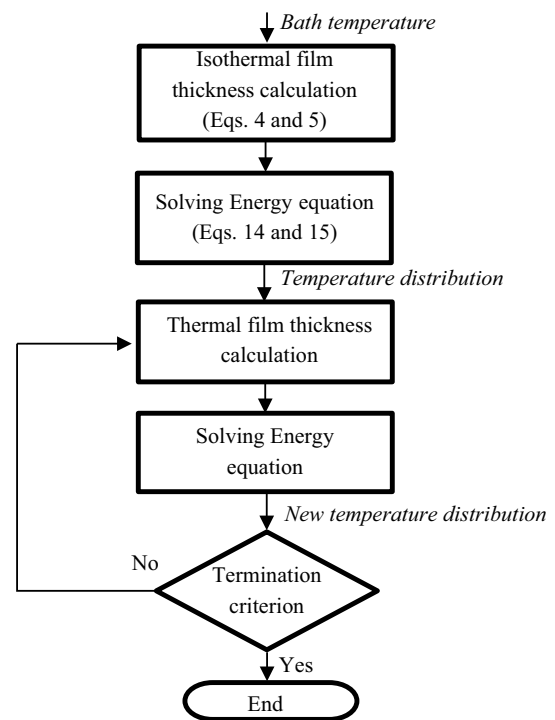


Fig. 2 Flow chart for calculating thermal film thickness

are used to solve the energy Eqs. (14, 15) and find a new temperature distribution. Then, the viscosity of each point is updated with this temperature field to start an iterative solving process that gives the thermal film thickness and the temperature distribution. The termination criterion of this process is defined as a difference below 0.1 nm in the film thickness calculated in two consecutive iterations.

3 Relevance of the Thermal Effects on Film Thickness

The described methodology for numerically solving the thermal EHL problem has been applied to a typical lubricant under EHL operating conditions [8]: steel–steel contact with $R = 0.02$ m, $p_m = 0.8$ GPa, $u_m = 1$ m/s, $\mu_0 = 0.08$ Pa s, $\alpha = 15$ GPa⁻¹, $\beta = 0.076$ K⁻¹, $G = 10$ MPa, $n = 0.75$, $k_1 = 0.1515$ W/m K, $\rho_1 = 975$ kg/m³, $c_1 = 2000$ J/kg K. Figure 3 shows temperature distributions of the lubricant and the contacting surfaces in two cases: low slide-to-roll ratio ($\Sigma = 0.5$) and medium slide-to-roll ratio ($\Sigma = 1.0$).

The thermal solving process has been performed for the two Reynolds–Carreau equations presented in references [8, 10]. In both cases, analogous temperature distributions are attained. Hence, the results are shown only for the new model (Eq. 4).

As the SRR increases, more heat is generated in the inlet zone due to the difference in velocities between the layers

of fluid. For a low slide-to-roll ratio ($\Sigma = 0.5$), the inlet temperature is 10% higher to that of the lubricant bath, there being a 34% jump in the case of a medium slide-to-roll ratio ($\Sigma = 1.0$), something which shows how important it is to include the energy equation during the resolution when the SRR reaches significant values. As far as film thickness is concerned, the rise in SRR causes an increasing loss of viscosity due to the pseudoplastic and thermal effects on the lubricant, with the ensuing reduction in film thickness (Fig. 3). These results are in line with references [21, 22].

4 New Film Thickness Formula

A new film thickness formula is determined from the results of the aforementioned Reynolds–Carreau equations [8, 10] for the thermal case. The process aims to obtain easy-to-use expressions following a methodology used by Anuradha and Kumar in [2], to which a new thermal factor is added. This process consists of the following stages:

- Selecting the range of input parameters and the types of equations to fit.
- Fitting an equation for the Newtonian film thickness h_N .
- Fitting a factor to incorporate the shear-thinning effect under pure rolling conditions: φ_{NN} .
- Fitting a factor to incorporate the shear-thinning effect under rolling and sliding conditions: φ_{SRR} .

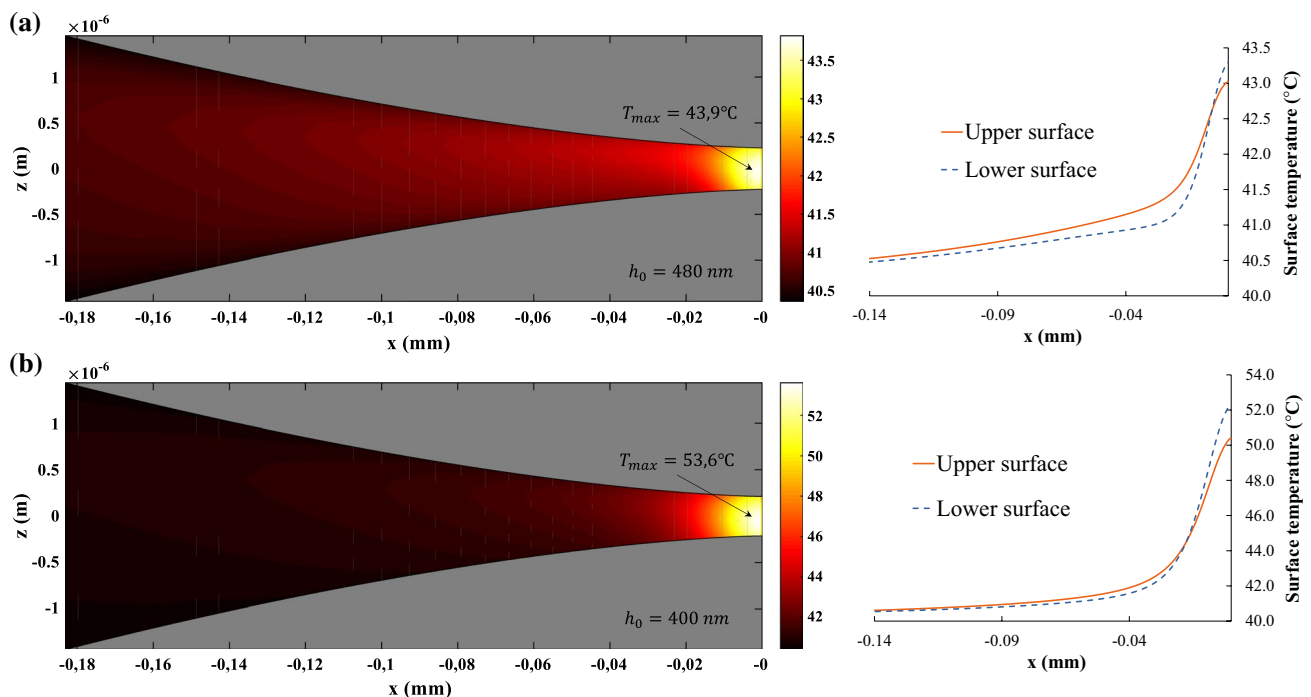


Fig. 3 Film thickness and temperature distribution of the lubricant and the upper/faster surface and the lower/slower surface. **a** $\Sigma = 0.5$; **b** $\Sigma = 1.0$

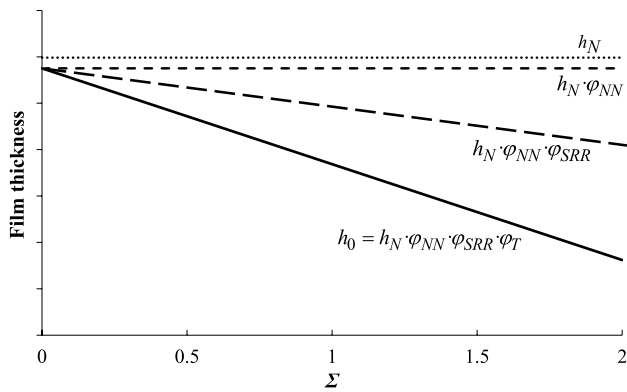


Fig. 4 Influence of the correction factors on the film thickness

Table 1 Range of input dimensionless parameters

Dimensionless parameter	Range
\bar{U}	$[4.93 \times 10^{-13}, 9.86 \times 10^{-12}]$
\bar{W}	$[1.46 \times 10^{-4}, 5.14 \times 10^{-4}]$
\bar{G}	[3989, 7132]
G/E'	$[1.42 \times 10^{-6}, 4.74 \times 10^{-5}]$
n	[0.3, 1.0]
Σ	[0, 1.5]

- Fitting a thermal correction factor for film thickness: φ_T .

Figure 4 outlines the effect of each of the factors in a film thickness versus SRR graph. When using all the factors, the film thickness is obtained with Eq. (20)

$$h_0 = h_N \cdot \varphi_{NN} \cdot \varphi_{SRR} \cdot \varphi_T \tag{20}$$

Expressions are presented as a function of the usual dimensionless parameters for velocity \bar{U} , load \bar{W} , material \bar{G} and Newtonian limit G/E' . Based on [2], the range of input dimensionless parameters used for determining the equations is shown in Table 1.

Several materials with different mechanical and thermal properties are considered in order to obtain more general equations, with a broader range of applicability.

For the Newtonian film thickness, the equation model is (21), where k_1 – k_4 are adjustable constants to be obtained

$$\frac{h_N}{R} = k_1 \bar{U}^{k_2} \bar{G}^{k_3} \bar{W}^{k_4} \tag{21}$$

After fitting the Newtonian formula, Eq. (22) provides a shear-thinning correction under pure rolling conditions,

$$\varphi_{T,New} = \frac{1 - 424.4448 \frac{p_m}{E'} \left(\frac{\mu_0 \mu_m^2}{\beta T_b^2 k_1} \right)^{0.3053} \left(\frac{k_b}{k_1} \right)^{-1.0458} \left(\frac{G}{E'} \right)^{0.0195n} \left(\frac{c_b}{c_1} \right)^{-3.5064} \left(\frac{\rho_l}{\rho_b} \right)^{0.0492}}{1 + 6.4127 \left(1 + 1.3148 \Sigma^{1.6814} \right) \left(\frac{\mu_0 \mu_m^2}{\beta T_b^2 k_1} \right)^{0.6098}} \tag{28}$$

where k_5 – k_{11} are constants to be adjusted. This expression is based on the non-Newtonian viscosity corrector of Carreau

$$\varphi_{NN} = \left(1 + k_5 \frac{\bar{U}^{k_6} \bar{W}^{k_7}}{\bar{G}^{k_8} (G/E')^{k_9}} \right)^{k_{10}(1-n)^{k_{11}}} \tag{22}$$

As for the shear-thinning correction factor under rolling and sliding conditions, a similar type of equation is considered (23), but taking into account SRR:

$$\varphi_{SRR} = \left(1 + k_{12} \frac{\Sigma^{k_{13}} \bar{U}^{k_{14}} \bar{W}^{k_{15}}}{\bar{G}^{k_{16}} (G/E')^{k_{17}}} \right)^{k_{18}(1-n)^{k_{19}}} \tag{23}$$

It is worth noting that both φ_{NN} and φ_{SRR} are equal to one for the Newtonian case ($n = 1$).

To take account of the film thickness reduction due to thermal effects, the equation used (24) is based on the empirical expression (11). In order to broaden the application range, additional factors are added, such as thermal conductivity, specific heat and density of the contacting bodies

$$\varphi_T = \frac{1 - k_{20} \frac{p_m}{E'} \left(\frac{\mu_0 \mu_m^2}{\beta T_b^2 k_1} \right)^{k_{21}} \left(\frac{k_b}{k_1} \right)^{k_{22}} \left(\frac{G}{E'} \right)^{k_{23}n} \left(\frac{c_b}{c_1} \right)^{k_{24}} \left(\frac{\rho_l}{\rho_b} \right)^{k_{25}}}{1 + k_{26} \left(1 + k_{27} \Sigma^{k_{28}} \right) \left(\frac{\mu_0 \mu_m^2}{\beta T_b^2 k_1} \right)^{k_{29}}} \tag{24}$$

The constants in Eqs. (21–24) are determined by using the GRG algorithm [23] to minimise the sum of squared deviations of the fitted equation with respect to the results of the simulations using Reynolds–Carreau equations with thermal effects.

In this way, the fitted expression for Newtonian film thickness is presented in Eq. (25). Likewise, Eqs. (26–28) show the corresponding correction factors obtained when performing thermal calculations with the new model described by the authors in [10]

$$\frac{h_N}{R} = 1.9983 \bar{U}^{0.7376} \bar{G}^{0.7385} \bar{W}^{-0.1091} \tag{25}$$

$$\varphi_{NN,New} = \left(1 + \frac{\bar{U}^{0.3960} \bar{W}^{0.2212}}{\bar{G}^{1.3541} (G/E')^{1.7724}} \right)^{-0.9447(1-n)^{1.6978}} \tag{26}$$

$$\varphi_{SRR,New} = \left(1 + 0.2335 \frac{\Sigma^{1.0620} \bar{U}^{0.1045} \bar{W}^{0.2706}}{\bar{G}^{0.5225} (G/E')^{0.5150}} \right)^{-36.8638(1-n)} \tag{27}$$

Table 2 Film thickness results for the new Reynolds–Carreau model

p_m (GPa)	u_m (m/s)	Σ	$h_{0,New}$ numerical (nm)	$h_{0,New}$ formula (nm)	Error (%)
0.8	0.13	0	191	192	0.5
0.8	0.50	0	503	500	-0.6
0.8	1.00	0	813	806	-0.9
0.8	1.50	0	1063	1056	-0.7
0.8	2.00	0	1274	1271	-0.2
0.8	2.60	0	1485	1495	0.7
1.5	0.13	0	163	164	0.6
1.5	0.50	0	425	422	-0.7
1.5	1.00	0	681	671	-1.5
1.5	1.50	0	884	869	-1.7
1.5	2.00	0	1053	1035	-1.7
1.5	2.60	0	1221	1205	-1.3
0.8	0.13	0.25	181	187	3.2
0.8	0.50	0.25	484	485	0.2
0.8	1.00	0.25	784	779	-0.6
0.8	1.50	0.25	1026	1018	-0.8
0.8	2.00	0.25	1229	1222	-0.6
0.8	2.60	0.25	1434	1434	0.0
1.5	0.13	0.25	148	159	6.9
1.5	0.50	0.25	397	405	2.0
1.5	1.00	0.25	641	641	0.0
1.5	1.50	0.25	836	827	-1.1
1.5	2.00	0.25	996	982	-1.4
1.5	2.60	0.25	1157	1139	-1.6
1.5	0.13	0.75	149	147	-1.4
1.5	0.50	0.75	384	368	-4.3
1.5	1.00	0.75	595	575	-3.5
1.5	1.50	0.75	693	733	5.5
1.5	2.00	0.75	862	861	-0.1
1.5	2.60	0.75	964	987	2.3

Steel–steel contact with $R = 0.1$ m, $\mu_0 = 0.08$ Pa s, $\alpha = 18.9$ GPa⁻¹, $\beta = 0.076$ K⁻¹, $T_b = 313$ K, $G = 0.3$ MPa, $n = 0.8$, $k_1 = 0.15$ W/m K, $\rho_1 = 975$ kg/m³, $c_1 = 2000$ J/kg K

An advantage of the structure of these equations is that all the factors are completely independent. Therefore, they can be applied in any order.

Table 2 compares the film thickness results obtained using expressions (25–28) “ $h_{0,New}$ formula”, with the equivalent results calculated numerically with the new Reynolds–Carreau equation “ $h_{0,New}$ numerical”, showing an average error lower than 2%. This indicates that the fitting process followed leads to a very good agreement between the adjusted formula and the numerical results.

On the other hand, analogous Eqs. (29, 30) are obtained for the shear-thinning factors from the Reynolds–Carreau equation proposed by Bair [8]. However, identical equations are considered to obtain the Newtonian film thickness (25)

Table 3 Film thickness results for the model proposed by Bair

p_m (GPa)	u_m (m/s)	Σ	$h_{0,Bair}$ numerical (nm)	$h_{0,Bair}$ formula (nm)	Error (%)
0.8	0.13	0	182	187	2.7
0.8	0.50	0	479	482	0.6
0.8	1.00	0	777	772	-0.7
0.8	1.50	0	1017	1007	-1.0
0.8	2.00	0	1224	1207	-1.4
0.8	2.60	0	1432	1415	-1.2
1.5	0.13	0	155	159	2.8
1.5	0.50	0	405	403	-0.4
1.5	1.00	0	651	635	-2.4
1.5	1.50	0	850	816	-4.0
1.5	2.00	0	1016	966	-4.9
1.5	2.60	0	1182	1115	-5.6
0.8	0.13	0.25	180	183	1.6
0.8	0.50	0.25	463	461	-0.5
0.8	1.00	0.25	734	725	-1.3
0.8	1.50	0.25	946	932	-1.5
0.8	2.00	0.25	1119	1104	-1.4
0.8	2.60	0.25	1288	1277	-0.8
1.5	0.13	0.25	152	155	1.9
1.5	0.50	0.25	387	382	-1.4
1.5	1.00	0.25	605	587	-2.9
1.5	1.50	0.25	771	742	-3.7
1.5	2.00	0.25	904	866	-4.2
1.5	2.60	0.25	1031	985	-4.5
1.5	0.13	0.75	148	151	1.9
1.5	0.50	0.75	366	362	-1.0
1.5	1.00	0.75	560	546	-2.5
1.5	1.50	0.75	704	678	-3.7
1.5	2.00	0.75	816	779	-4.6
1.5	2.60	0.75	919	871	-5.2

Steel–steel contact with $R = 0.1$ m, $\mu_0 = 0.08$ Pa s, $\alpha = 18.9$ GPa⁻¹, $\beta = 0.076$ K⁻¹, $T_b = 313$ K, $G = 0.3$ MPa, $n = 0.8$, $k_1 = 0.15$ W/m K, $\rho_1 = 975$ kg/m³, $c_1 = 2000$ J/kg K

and the thermal correction factor (28), as they are not influenced by the model in Ref. [8]

$$\varphi_{NN,New}^{Bair} = \left(1 + 3.5061 \times 10^{-8} \frac{\bar{U}^{0.6902} \bar{W}^{0.3495}}{\bar{G}^{2.0181} (G/E')^{4.4027}} \right)^{-0.1199(1-n)} \tag{29}$$

$$\varphi_{SRR,New}^{Bair} = \left(1 + 4.2163 \times 10^{-6} \frac{\Sigma^{0.6235} \bar{U}^{0.5256} \bar{W}^{0.1918}}{\bar{G}^{1.7568} (G/E')^{3.0968}} \right)^{-1.6580(1-n)} \tag{30}$$

By comparing the results of this model with those of the model proposed in [10], average deviations of lower than 3% are found (Table 3). The numerical results presented are attained by means of the calculation process described

in the present article in order to obtain results that can be compared.

5 Results of the New Formula and the New Factors

Having verified that the new formula provides results equivalent to those of the numerical simulations within the range specified in Table 1, the new correction factors for shear-thinning and thermal effects have been compared with results of other authors.

Table 4 compares several film thickness corrections due to shear-thinning under isothermal conditions for the model proposed by Bair (Eqs. 29, 30), Anuradha and Kumar (Eqs. 8, 9) and the new Eqs. (26, 27). The correlation between the new formulae and those of Anuradha and Kumar “A&K” is shown in Fig. 5 and in the last column of Table 4, with percentage differences less than 20% in all cases (usually less than 10%). These variations are explained by the fact that Newtonian film thickness differs from one model to another, as noted in references [7, 10]. Indeed, Anuradha and Kumar tend to obtain a lower Newtonian film thickness and therefore the corresponding factors apply a

lesser shear-thinning correction to match the numerical simulations, leading to negative differences in most cases.

In Table 5 and Fig. 6, the thermal factor (11) is compared with the new formula (28). Both expressions give similar results (differences lower than 9%), with values slightly higher for the new factor. Hence, the new model predicts a less significant thermal influence on film thickness.

After the analysis of the individual effect of shear-thinning and thermal factors, film thickness calculations have been done taking into account all the factors. Figure 7 shows the results of the formulae developed for the Bair model (Eqs. 25, 28, 29, 30) and the new formula (Eqs. 25, 26, 27, 28), together with the results of Anuradha and Kumar (Eqs. 6, 8, 9) modified with the thermal factor of Eq. (11) to be able to compare the predictions [denoted by “A&K + Eq. (11)”].

The results of the film thickness formula developed for the new model present a clear agreement with those of Anuradha and Kumar throughout the range compared, showing average deviations of 12% and a similar decreasing trend as SRR rises. This is in line with the simulations presented in the article [10] for the isothermal case, where the new model shows a film thickness variation with SRR close to the results of Anuradha and Kumar, which are based on full

Table 4 Film thickness corrections due to shear-thinning under isothermal conditions

p_m (GPa)	u_m (m/s)	Σ	κ^{-1}	$\varphi_{NN,New}^{Bair} \times \varphi_{SRR,New}^{Bair}$	$\bar{R} \times \bar{S}$	$\varphi_{NN,New} \times \varphi_{SRR,New}$	Difference (%)
0.8	0.13	0.75	0.835	0.990	0.866	0.830	- 4.4
0.8	0.50	0.75	0.776	0.978	0.843	0.792	- 6.4
0.8	2.00	0.75	0.700	0.951	0.806	0.742	- 8.6
0.8	2.60	0.75	0.683	0.944	0.797	0.731	- 9.0
1.0	0.13	0.75	0.826	0.989	0.865	0.811	- 6.7
1.0	0.50	0.75	0.764	0.975	0.840	0.771	- 9.0
1.0	2.00	0.75	0.685	0.946	0.800	0.717	- 11.6
1.0	2.60	0.75	0.668	0.938	0.790	0.705	- 12.0
1.5	0.13	0.75	0.807	0.986	0.861	0.772	- 11.6
1.5	0.50	0.75	0.741	0.969	0.832	0.726	- 14.7
1.5	2.00	0.75	0.656	0.934	0.786	0.666	- 18.0
1.5	2.60	0.75	0.639	0.925	0.774	0.653	- 18.6
0.8	0.13	1.5	0.746	0.988	0.629	0.704	10.6
0.8	0.50	1.5	0.675	0.974	0.603	0.656	8.0
0.8	2.00	1.5	0.591	0.943	0.568	0.596	4.7
0.8	2.60	1.5	0.573	0.935	0.560	0.584	4.0
1.0	0.13	1.5	0.734	0.987	0.630	0.673	6.5
1.0	0.50	1.5	0.661	0.971	0.603	0.622	3.2
1.0	2.00	1.5	0.575	0.937	0.566	0.560	- 0.9
1.0	2.60	1.5	0.557	0.928	0.557	0.547	- 1.8
1.5	0.13	1.5	0.712	0.983	0.630	0.613	- 2.9
1.5	0.50	1.5	0.635	0.964	0.601	0.557	- 7.9
1.5	2.00	1.5	0.546	0.924	0.559	0.490	- 13.9
1.5	2.60	1.5	0.528	0.914	0.549	0.477	- 15.2

Steel–steel contact with $R = 0.1$ m, $\mu_0 = 0.08$ Pa s, $\alpha = 18.9$ GPa⁻¹, $G = 1.0$ MPa, $n = 0.3$

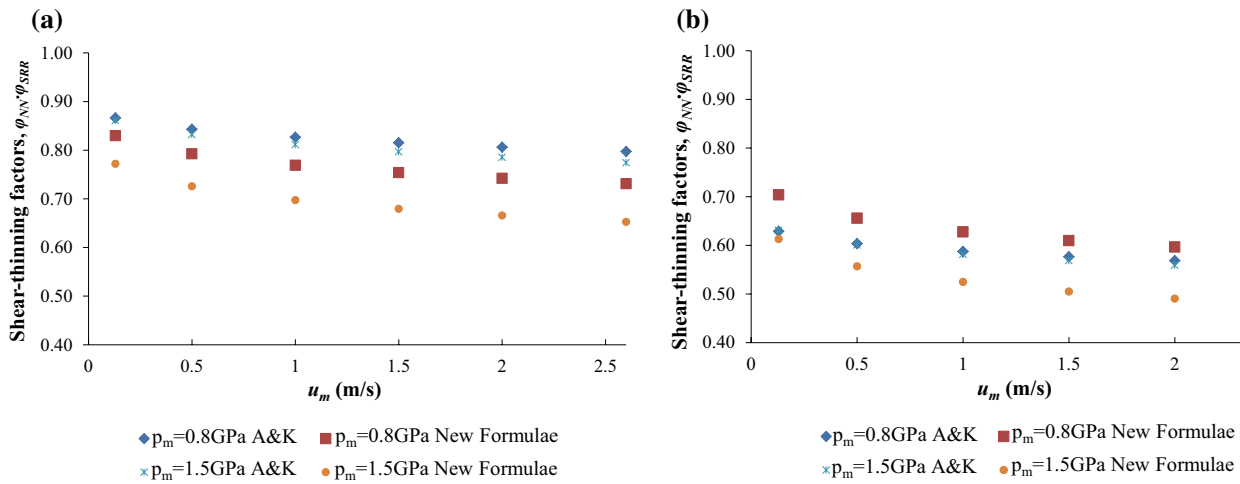


Fig. 5 Comparison of shear-thinning factors under isothermal conditions. Steel–steel contact with $R = 0.1$ m, $\mu_0 = 0.08$ Pa s, $\alpha = 18.9$ GPa⁻¹, $G = 1.0$ MPa, $n = 0.3$. **a** $\Sigma = 0.75$; **b** $\Sigma = 1.5$

Table 5 Film thickness corrections due to thermal effects

p_m (GPa)	u_m (m/s)	Σ	ϕ_T	$\phi_{T,New}$	Difference (%)
0.8	0.13	0.75	0.992	0.984	- 0.7
0.8	0.50	0.75	0.961	0.957	- 0.4
0.8	2.00	0.75	0.821	0.864	5.2
0.8	2.60	0.75	0.767	0.830	8.1
1.0	0.13	0.75	0.991	0.981	- 1.0
1.0	0.50	0.75	0.959	0.950	- 0.9
1.0	2.00	0.75	0.815	0.848	4.1
1.0	2.60	0.75	0.760	0.812	6.8
1.5	0.13	0.75	0.989	0.973	- 1.6
1.5	0.50	0.75	0.953	0.932	- 2.2
1.5	2.00	0.75	0.799	0.809	1.2
1.5	2.60	0.75	0.742	0.767	3.4
0.8	0.13	1.5	0.989	0.982	- 0.7
0.8	0.50	1.5	0.947	0.943	- 0.4
0.8	2.00	1.5	0.763	0.805	5.6
0.8	2.60	1.5	0.697	0.756	8.4
1.0	0.13	1.5	0.988	0.979	- 1.0
1.0	0.50	1.5	0.945	0.936	- 0.9
1.0	2.00	1.5	0.757	0.790	4.4
1.0	2.60	1.5	0.690	0.739	7.1
1.5	0.13	1.5	0.986	0.971	- 1.6
1.5	0.50	1.5	0.939	0.919	- 2.2
1.5	2.00	1.5	0.742	0.754	1.6
1.5	2.60	1.5	0.674	0.699	3.7

Steel–steel contact with $R = 0.1$ m, $\mu_0 = 0.08$ Pa s, $\alpha = 18.9$ GPa⁻¹, $\beta = 0.076$ K⁻¹, $T_b = 313$ K, $G = 1.0$ MPa, $n = 0.3$, $k_1 = 0.15$ W/m K, $\rho_l = 975$ kg/m³, $c_l = 2000$ J/kg K

EHL simulations. In contrast, the formula obtained for the Bair model shows lower sensitivity to SRR.

Bearing in mind the lack of film thickness measurements for line contacts, it is interesting to compare the results of the new formula with experimental data under thermal conditions, Ref. [24]. For this purpose, approximate values of the rheological parameters have been taken (Table 6), utilising information available for lubricants of a similar nature.

Figure 8 depicts the calculated film thickness as a function of SRR for diverse lubricants, together with the experimental results. In these cases, the input parameters move away from the range specified in Table 1 and the new formula only allows a rough estimate. The results can be improved by using a more general Newtonian formula instead of Eq. (25), such as the Hamrock formula for line contact [6]:

$$h_{Nc} = 2.154\alpha^{0.47}(\mu_0 u_m)^{0.692} E'^{0.110} R^{0.308} p_0^{-0.332} \quad (31)$$

Figure 8 also presents the predictions attained by applying the new correction factors in Eqs. (26–28) to the Hamrock formula. The results show a better agreement with the experimental data, and the new correction factors properly estimate the variation of film thickness with regard to SRR and lubricant type.

6 Conclusions

The authors have improved their previous model to determine film thickness by considering thermal effects in the calculation process of the Reynolds–Carreau equation. Solving

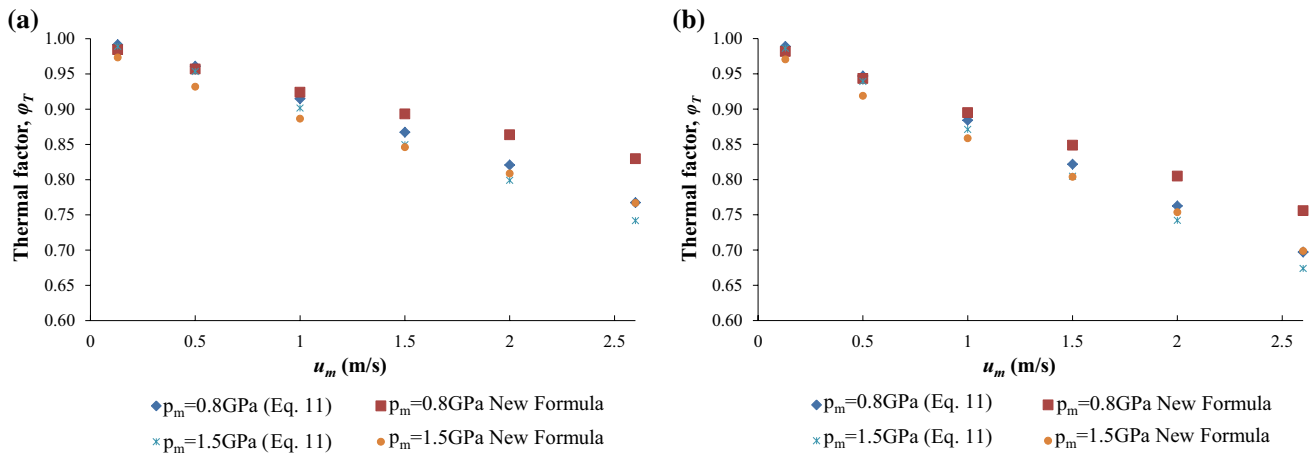


Fig. 6 Comparison of thermal factors. Steel–steel contact with $R = 0.1$ m, $\mu_0 = 0.08$ Pa s, $\alpha = 18.9$ GPa $^{-1}$, $\beta = 0.076$ K $^{-1}$, $T_b = 313$ K, $G = 1.0$ MPa, $n = 0.3$, $k_1 = 0.15$ W/m K, $\rho_1 = 975$ kg/m 3 , $c_1 = 2000$ J/kg K. **a** $\Sigma = 0.75$; **b** $\Sigma = 1.5$

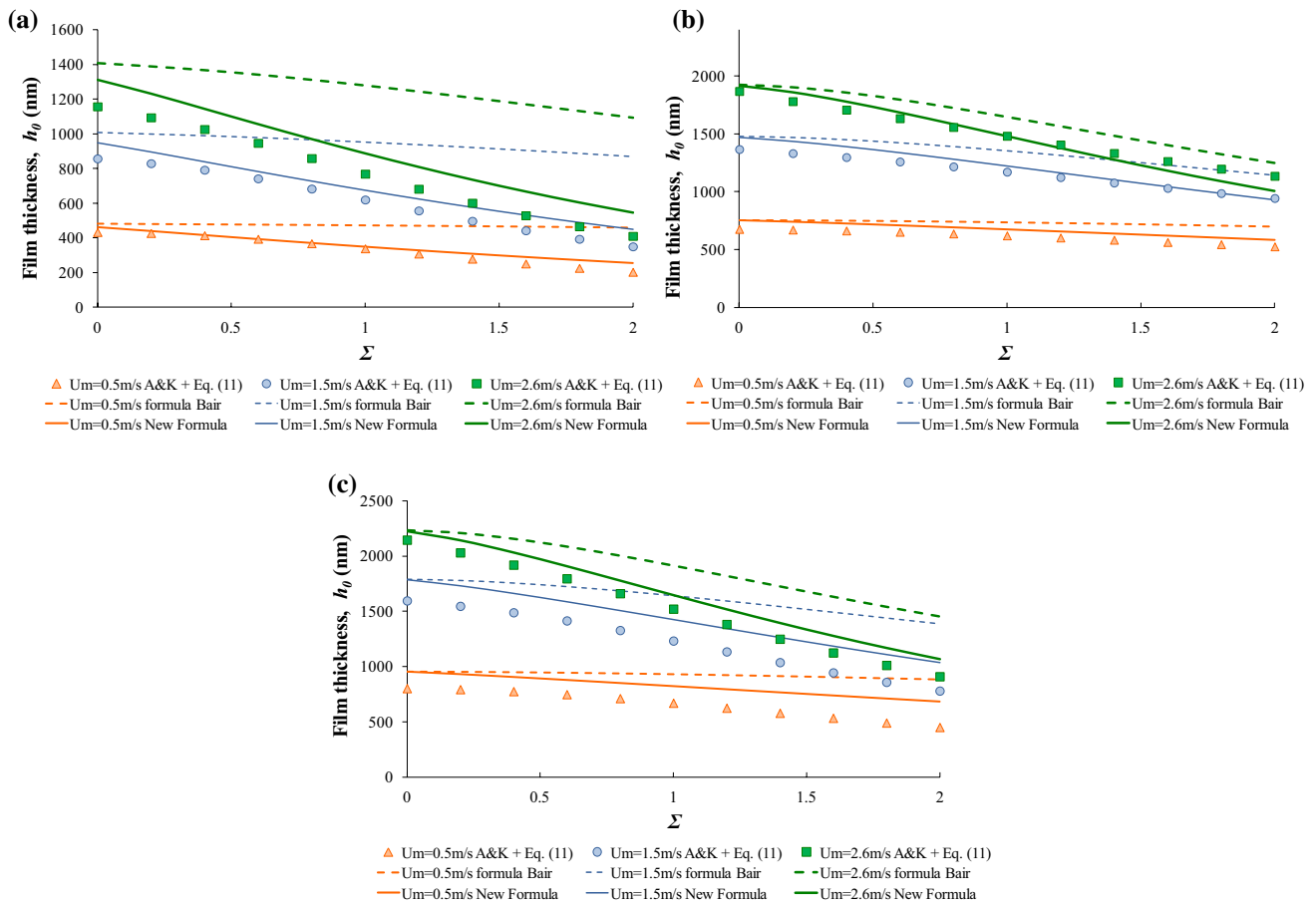


Fig. 7 Film thickness calculations using different formulae. Steel–steel contact with $R = 0.1$ m, $k_1 = 0.15$ W/m K, $c_1 = 2000$ J/kg K. **a** $p_m = 1.0$ GPa, $\mu_0 = 0.08$ Pa s, $\alpha = 18.9$ GPa $^{-1}$, $\beta = 0.076$ K $^{-1}$, $T_b = 313$ K, $G = 1.0$ MPa, $n = 0.3$, $\rho_1 = 975$ kg/m 3 ; **b** base oil

M100, $T_b = 298$ K, $p_m = 1.5$ GPa, $\rho_1 = 900$ kg/m 3 ; **c** base oil N100, $T_b = 298$ K, $p_m = 2.0$ GPa, $\rho_1 = 900$ kg/m 3 . The parameters of these base oils are given in Table 6

Table 6 Rheological parameters considered for the lubricants

Lubricant	Composition	Kinematic viscosity (mm ² /s) [24]	α (GPa ⁻¹) [24]	n [6]	G (MPa) [6]
PAO	Polyalphaolefin	94.1 at 40 °C	16.8 at 25 °C	0.40	6.0
		14.0 at 100 °C	12.4 at 100 °C		
M100	Paraffinic oil	96.0 at 40 °C	22.0 at 25 °C	0.65	3.5
		10.6 at 100 °C	15.8 at 100 °C		
N100	Naphthenic oil	97.9 at 40 °C	32.5 at 25 °C	0.34	5.6
		8.6 at 100 °C	20.6 at 100 °C		

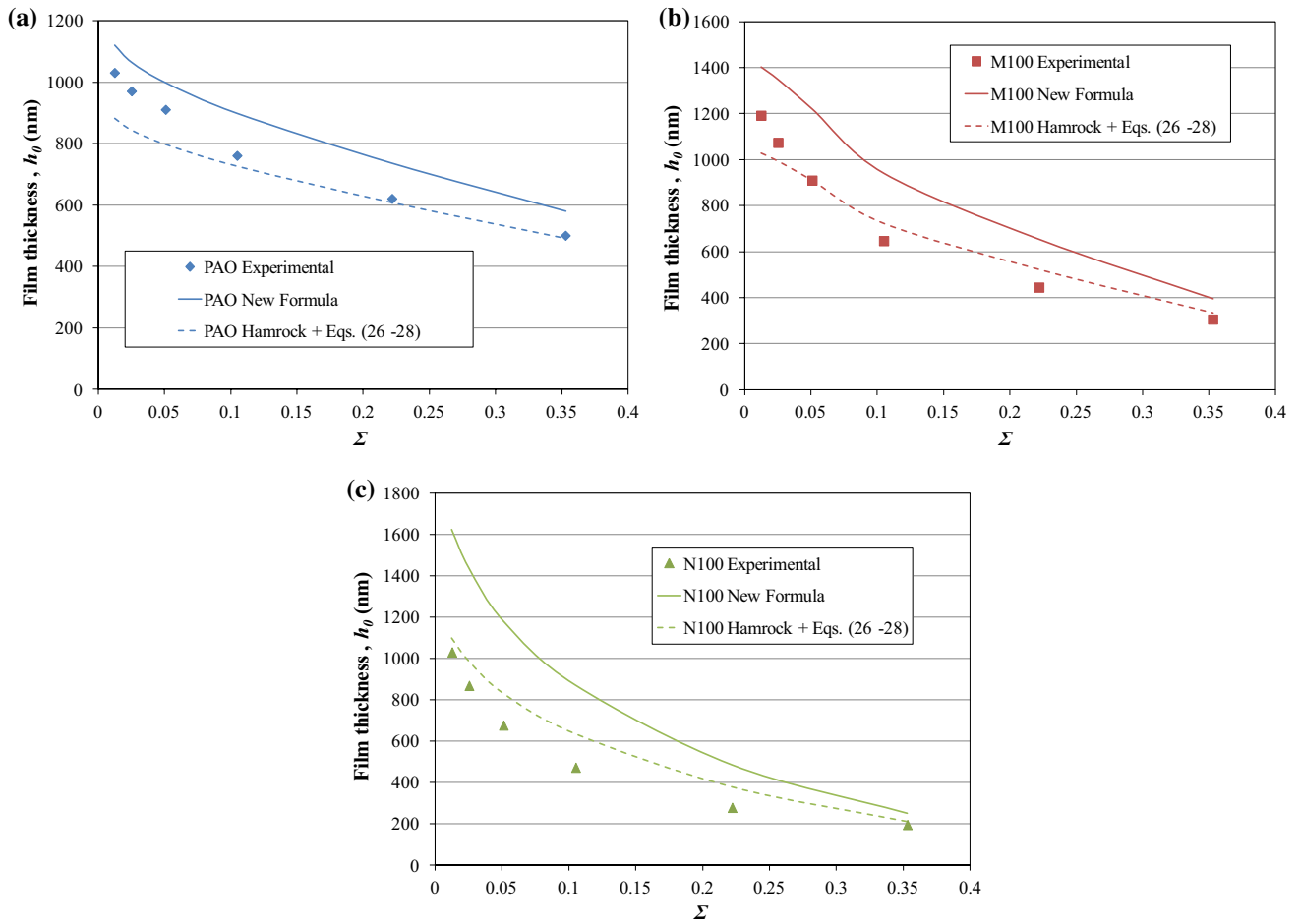


Fig. 8 Comparison between predicted results and experimental data from Ref. [24]. Steel–steel contact with $p_m = 0.785$ GPa, $u_m = 8$ m/s, $R = 0.02$ m, $k_1 = 0.15$ W/m K, $\rho_1 = 900$ kg/m³, $c_1 = 2000$ J/kg K. **a** PAO; **b** M100; **c** N100

the energy equation has allowed for the determination of the temperature distributions in the lubricant and the contacting surfaces in the inlet zone. In this way, the results with different working conditions have been discussed.

As a result of the application of the model developed over a wide range of conditions, a new film thickness formula is

proposed for EHL line contacts, which can be used for fast and easy calculations. The new formula consists of an equation for the Newtonian film thickness, a shear-thinning factor under pure rolling, a shear-thinning factor under rolling and sliding conditions and a thermal factor:

$$\frac{h_N}{R} = 1.9983 \bar{U}^{0.7376} \bar{G}^{0.7385} \bar{W}^{-0.1091}$$

$$\varphi_{NN,New} = \left(1 + \frac{\bar{U}^{0.3960} \bar{W}^{0.2212}}{\bar{G}^{1.3541} (G/E')^{1.7724}} \right)^{-0.9447(1-n)^{1.6978}}$$

$$\varphi_{SRR,New} = \left(1 + 0.2335 \frac{\Sigma^{1.0620} \bar{U}^{0.1045} \bar{W}^{0.2706}}{\bar{G}^{0.5225} (G/E')^{0.5150}} \right)^{-36.8638(1-n)}$$

$$\varphi_{T,New} = \frac{1 - 424.4448 \frac{\rho_m}{E'} \left(\frac{\mu_0 u_m^2}{\beta T_b^2 k_1} \right)^{0.3053} \left(\frac{k_b}{k_1} \right)^{-1.0458} \left(\frac{G}{E'} \right)^{0.0195n} \left(\frac{c_b}{c_1} \right)^{-3.5064} \left(\frac{\rho_l}{\rho_b} \right)^{0.0492}}{1 + 6.4127 \left(1 + 1.3148 \Sigma^{1.6814} \right) \left(\frac{\mu_0 u_m^2}{\beta T_b^2 k_1} \right)^{0.6098}}$$

Therefore, the complete film thickness equation can be expressed as follows

$$h_0 = h_N \cdot \varphi_{NN} \cdot \varphi_{SRR} \cdot \varphi_T$$

This expression has shown to provide reasonably good accuracy for predicting the film thickness when compared to numerical calculations using Reynolds–Carreau equations, to full EHL simulations and to experimental results.

Acknowledgements This work was carried out as a part of the Research Project DPI2013-48348-C2-2-R, financed by the Spanish Ministry of Economy and Competitiveness. We would also like to thank the Lubricants Laboratory of Repsol.

References

- Jang, J.Y., Khonsari, M.M., Bair, S.: On the elastohydrodynamic analysis of shear-thinning fluids. *Proc. R. Soc. A* **463**, 3271–3290 (2007)
- Anuradha, P., Kumar, P.: New film thickness formula for shear thinning fluids in thin film elastohydrodynamic lubrication line contacts. *Proc. Inst. Mech. Eng. Part J: J. Eng. Tribol.* **225**, 173–179 (2011)
- Carreau, P.J.: Rheological equations from molecular network theories. *Trans. Soc. Rheol.* **16**(1), 99–127 (1972)
- Bair, S.: A Reynolds–Ellis equation for line contact with shear-thinning. *Tribol. Int.* **39**, 310–316 (2002)
- Bair, S., Vergne, P., Querry, M.: A unified shear-thinning treatment of both film thickness and traction in EHD. *Tribol. Lett.* **18**(2), 145–152 (2005)
- Bair, S.: High pressure rheology for quantitative elastohydrodynamics. In: Bair, S., McCabe, C. (eds) *Tribology and Interface Engineering Series*. No 54 ed. Elsevier, London (2007)
- De la Guerra, E., Echávarri, J., Chacón, E., Lafont, P., Díaz, A., Muñoz-Guijosa, J.M., Muñoz, J.L.: New Reynolds equation for line contact based on the Carreau model modification by Bair. *Tribol. Int.* **55**, 141–147 (2012)
- Bair, S., Khonsari, M.M.: Reynolds equation for common generalized Newtonian model and an approximate Reynolds–Carreau equation. *Proc. Inst. Mech. Eng. Part J: J. Eng. Tribol.* **220**(4), 365–374 (2006)
- Grubin, A.N.: *Fundamentals of the hydrodynamic theory of lubrication of heavily loaded cylindrical surfaces*. Book No. 30 (1949), Central Scientific Research Institute for Technology and Mechanical Engineering, Moscow (DSIR Translation)
- De la Guerra, E., Echávarri, J., Sánchez, A., Chacón, E.: Film thickness predictions for line contact using a new Reynolds–Carreau equation. *Tribol. Int.* **82**, 133–141 (2015)
- Habchi, W., Vergne, P., Bair, S., Andersson, O., Eyheramendy, D., Morales-Espejel, G.E.: Influence of pressure and temperature dependence of thermal properties of a lubricant on the behavior of circular TEHD contacts. *Tribol. Int.* **43**, 1842–1850 (2010)
- Echávarri, J., Lafont, P., Chacón, E., de la Guerra, E., Díaz, A., Muñoz-Guijosa, J.M., Muñoz, J.L.: Analytical model for predicting the friction coefficient in point contacts with thermal elastohydrodynamic lubrication. *Proc. Inst. Mech. Eng. Part J: J. Eng. Tribol.* **225**, 181–191 (2011)
- Anuradha, P., Kumar, P.: New minimum film thickness formula for EHL rolling/sliding line contacts considering shear thinning behaviour. *Proc. Inst. Mech. Eng. Part J: J. Eng. Tribol.* **227**(3), 187–198 (2012)
- Carli, M., Sharif, K.J., Ciulli, E., Evans, H.P., Snidle, R.W.: Thermal point contact EHL analysis of rolling/sliding contacts with experimental comparison showing anomalous film shapes. *Tribol. Int.* **42**(4), 517–525 (2009)
- Spikes, H.A., Anghel, V., Glovnea, R.: Measurement of the rheology of lubricant films within elastohydrodynamic contacts. *Tribol. Lett.* **17**, 593–605 (2004)
- Habchi, W., Eyheramendy, D., Bair, S., Vergne, P., Morales-Espejel, G.: Thermal elastohydrodynamic lubrication of point contacts using a Newtonian/generalized Newtonian lubricant. *Tribol. Lett.* **30**, 41–52 (2008)
- Raisin, J., Fillot, N., Dureisseix, D., Vergne, P., Lacour, V.: characteristic times in transient thermal elastohydrodynamic line contacts. *Tribol. Int.* **82**, 472–483 (2015)
- Stachowiak, G.W., Batchelor, A.W.: *Engineering Tribology*. Elsevier, Oxford (2005)
- Wilson, W.R.D.: A Framework for thermohydrodynamic lubrication analysis. *J. Tribol.* **120**(2), 399–405 (1998)
- De la Guerra, E., Echávarri, J., Chacón, E., Del Río, B.: A thermal resistances-based approach for thermal-elastohydrodynamic calculations in point contacts. *Proc. Inst. Mech. Eng. Part C: J. Mech. Eng. Sci.* (2017). <https://doi.org/10.1177/0954406217713231>
- Hsiao, H.S., Hamrock, B.J.: A complete solution for thermal-elastohydrodynamic lubrication of line contacts using circular non-Newtonian fluid model. *J. TWM. ASME paper 91-Trib-24* (1992)
- Kumar, P., Anuradha, P., Khonsari, M.M.: Some important aspects of thermal elastohydrodynamic lubrication. *Proc. Inst. Mech. Eng. Part C: J. Mech. Eng. Sci.* **224**, 2588–2598 (2010)
- Abadie, J., Carpentier, J.: Generalization of the Wolfe reduced gradient method to the case of nonlinear constraints. In: Fletcher, R. (ed.) *Optimization*. Academic, New York (1969)
- Höhn, B.R., Michaelis, K., Mann, U.: Measurement of oil film thickness in elastohydrodynamic contacts influence of various base oils and VI-Improvers. *Tribol. Ser.* **31**, 225–234 (1996)